

# Determining the Galactic mass distribution using tidal streams from globular clusters

Chigurupati Murali & John Dubinski

Canadian Institute for Theoretical Astrophysics  
University of Toronto, Toronto, ON M5S 3H8, Canada

## ABSTRACT

We discuss how to use tidal streams from globular clusters to measure the mass distribution of the Milky Way. Recent proper motion determinations for globular clusters from plate measurements and Hipparcos astrometry provide several good candidates for Galactic mass determinations in the intermediate halo, far above the Galactic disk, including Pal 5, NGC 4147, NGC 5024 (M53) and NGC 5466; the remaining Hipparcos clusters provide candidates for measurements several kpc above and below the disk. These clusters will help determine the profile and shape of the inner halo. To aid this effort, we present two methods of mass determination: one, a generalization of rotation-curve mass measurements, which gives the mass and potential from complete position-velocity observations for stream stars; and another using a simple  $\chi^2$  estimator, which can be used when only projected positions and radial velocities are known for stream stars. We illustrate the use of the latter method using simulated tidal streams from Pal 5 and find that fairly accurate mass determinations are possible for relatively poor data sets, although current proper motion uncertainties represent the limiting factor. Follow-up observations of clusters with proper motion determinations may reveal tidal streams; obtaining radial velocity measurements can give useful measurements of the mass distribution in the inner Galaxy.

*Subject headings:* Galaxy: structure – Galaxy: halo – globular clusters – Galaxy: kinematics and dynamics – astrometry

## 1. Introduction

There are currently several important problems and related disputes which depend on our understanding of the mass distribution in the Galaxy. In the inner Galaxy, the *maximum disk* controversy revolves around determining the relative contributions of disk and halo to the measured rotation curve (e.g. Debattista & Sellwood 1998; Tremaine & Ostriker 1998). The measurement of the rotation curve is itself controversial (Olling & Merrifield 1998). At intermediate distances in the halo, the interpretation of microlensing searches for dark matter candidates depends fairly strongly on the shape of the Galaxy (Alcock et al 1997). Finally, cosmological models make strong

predictions for global halo structure (e.g. Dubinski & Carlberg 1991; Navarro, Frenk & White 1997). These results help fuel maximum disk arguments but also predict the shape of the halo at large distances. Resolving these issues requires significant improvements in our understanding of the mass distribution in the Galaxy.

A variety of methods have been used to estimate the mass of the Galaxy in different regions (see Fich & Tremaine 1991 for a review). In the inner Galaxy, estimates typically rely on measurements from observable material in the disk, including HI within the solar radius and open clusters, OB associations and planetary nebulae beyond the solar radius. Consequently, the mass distribution above and below the disk is relatively poorly known (Dehnen & Binney 1998). In the outer Galaxy, estimates typically rely on the dynamics of satellites and are subject to uncertainties regarding whether individual objects are bound to the Galaxy (e.g. Leo I) and whether or not the entire distribution is in equilibrium given the long orbital timescales (e.g. Little & Tremaine 1989; Kochanek 1996).

If we could perform experiments to determine the mass, we would choose an ensemble of test particles and study their motion in time under the influence of the Galactic gravitational field. Although we cannot do this, it has been pointed out that tidal streams trace orbits in the potential (e.g. Lynden-Bell 1982; Kuhn 1993; Johnston et al 1998), and can therefore be used to determine the mass distribution giving rise to that potential. In this sense, tidal streams are analogous to streak lines which are used to trace steady fluid flow (Batchelor 1967).

However, with the sole exception of the Magellanic stream— whose origin and dynamics remain controversial (Moore & Davis 1994)— full-fledged tidal streams remain unobserved. Nevertheless, there is an abundance of theoretical work which predicts the existence of tidal streams and other substructure, either from fully disrupted, infalling satellites (e.g. Tremaine 1993; Johnston, Hernquist & Bolte 1996) or from visible satellites such as globular clusters which undergo mass loss as they orbit in the Galaxy (e.g. Gnedin & Ostriker 1997; Murali & Weinberg 1997; Vesperini 1997). In addition, the hierarchical picture of structure formation predicts that Galactic halos should contain a significant amount of debris from accreted substructure, suggesting that the halo is filled with tidal streams (Johnston et al 1996).

Recent observations have finally begun to reveal traces of tidal streams and substructure in the Galactic stellar halo. The Sagittarius dwarf provides an archetype for satellite accretion (Ibata, Gilmore & Irwin 1994) and ongoing observations are attempting to reveal the associated stream (Mateo et al 1998). Other observations have revealed moving groups and phase space substructure (e.g. Majewski, Munn & Hawley 1996) and extra-tidal stars surrounding globular clusters (Grillmair et al 1995). Given proposed astrometric satellites, SIM and GAIA, the possibilities for using tidal streams to probe Galactic structure appear to have multiplied dramatically (Johnston et al 1998; Zhao et al 1999).

Given this motivation, we discuss in this paper the use of tidal streams from globular clusters, as suggested by Grillmair (1997), to probe the mass and potential of the Galaxy. Theoretical

work on cluster evolution (e.g. Gnedin & Ostriker 1997; Murali & Weinberg 1997; Vesperini 1997) suggests that globulars with mass  $M_c \lesssim 10^5 M_\odot$  and Galactocentric radius  $R_g \lesssim 20$  kpc will provide excellent candidates for stream measurements because they tend to lose mass through the combined effects of internal relaxation, tidal heating and post-collapse heating of the core. This suggests that many good candidates are available. We first summarize in §2 the dynamics of tidal streams created by mass loss from a satellite orbiting in an external potential. Then, in §3, we develop two methods for determining the Galactic mass and potential using tidal streams. Tests of these methods using Pal 5 as a model cluster and of the observational requirements are presented in §4. The interpretation and importance of the results as well as further possibilities are discussed in §5. In particular, we point out that recent proper motion determinations from plate measurements and Hipparcos data provide a sample of globular clusters which are good candidates for stream observations and mass determinations.

## 2. Dynamics of tidal streams

Mass loss from globular clusters is driven by a combination of internal relaxation, tidal heating and post-collapse heating of the core (e.g. most recently Gnedin & Ostriker 1997; Murali & Weinberg 1997; Vesperini 1997). Escaping stars reach the inner and outer Lagrange points nearly at rest and evaporate from the system. These particles have slight energy offsets from the center-of-mass of the system due to the small difference in potential energy determined by the finite size of the satellite (Tremaine 1993; Johnston 1998). The cluster center-of-mass energy  $E_c \sim \Phi_G(|R_c|)$ , the center-of-mass potential energy at perigalacticon; this defines a first-order, dimensionless energy correction for escaping stars:

$$\delta = \frac{\Phi_G(|R_c \pm r_t|) - \Phi_G(|R_c|)}{\Phi_G(|R_c|)} \approx \pm \frac{r_t}{R_c} \frac{d \ln |\Phi_G|}{d \ln R_c} \equiv \pm |\chi| \frac{r_t}{R_c}. \quad (1)$$

The parameter  $\delta = \epsilon/\Phi_G(R_c)$ , where  $\epsilon$  is the energy scale defined by Johnston (1998). The parameter  $|\chi| \leq 1$  ( $\chi = 1$  for a Kepler potential). For the typical globular clusters we will consider below,  $r_t \sim 50$  pc and  $R_c \sim 10$  kpc, so that  $\delta \sim 0.005$ ; i.e. less than a 1% correction. Therefore the mean motion of the stream is nearly indistinguishable from the center-of-mass of the satellite.

Johnston (1998) finds that the absolute energies of stripped material lies in the range  $0 - 2\delta$  and is sharply peaked about  $\delta$ . Thus the distribution of total energies lies in the range  $E_{com} \lesssim E_s \lesssim (1 + 2\delta)E_{com}$  (for positive  $\delta$ ). Therefore, the velocity spread in the stream falls in the range  $V_{com} \lesssim V_s \lesssim \sqrt{1 + 2\delta}V_{com}$ . For  $\delta = 0.005$  and  $V_{com} \sim 220$  km s<sup>-1</sup>, the velocity spread  $\Delta v \sim 1$  km s<sup>-1</sup>.

## 2.1. Simulated tidal streams

The phase space coordinates of individual stream stars are determined by the mass loss rate and fine-grained distribution of particle positions and velocities at the Lagrange points. Once particles are injected into the stream, they phase mix according to the collisionless Boltzmann equation; from the fine-grained evolution, one can calculate the velocity and density structure along the stream (Tremaine 1998; Helmi & White 1999).

Here we generate streams using both simple N-body simulations and an analytic approximation to the characteristics of the projected stream based on the discussion of energetics given above. In the quasistatic evolution of globular clusters, the mass loss rate is small so the potential remains very nearly spherical and constant over the timescales considered here. Therefore the N-body simulations use a fixed, Plummer-law satellite with test particle orbits integrated along the satellite’s orbit in the Galaxy.

With N-body calculations, it is difficult to accurately reproduce expected mass loss rates from globular clusters given the importance of internal relaxation and its dependence on the stellar mass spectrum as well as the possible importance of core heating in evaporating clusters (e.g. Gnedin & Ostriker 1997; Murali & Weinberg 1997). Therefore, to increase our flexibility, we adopt a simple Gaussian approximation to simulate the projected characteristics of tidal streams for use in the projected orbit fits discussed below. Of course, the dynamics of the stream are best studied through direct orbit integration and N-body simulation: below we compare this approximation with the results of a simulation to ensure that the approach is reasonable.

In this approximation, we adopt a mass loss rate to specify the number of stars in the stream and assume that the stream stars have Gaussian distributions of: 1) orbital phases about the current phase of the satellite; 2) line-of-sight, radial velocities about the line-of-sight, radial velocity of the satellite at the star’s phase; 3) angular offsets from the angular position of the satellite at the star’s phase. The phase distribution is very narrow for recent mass loss; this corresponds to a distribution clumped about the satellite. The phase distribution is very broad for mass loss in the distant past; this corresponds to a uniform phase distribution or a phase-mixed stream. The dispersion of the radial velocity distribution is given roughly by the velocity range determined from the energy spread. The angular dispersion corresponds to the angular size of the system at the star’s orbital phase.

In practice, we choose phase by sampling time along the orbit since azimuthal phase angle  $w = \Omega t$ , where  $\Omega$  is the azimuthal frequency of the orbit. The Galactic latitude of the satellite at this time is chosen as the phase variable <sup>1</sup>. Then radial velocity and angular variates are generated assuming means given by the center-of-mass coordinates at this phase. This provides a reasonable approximation for the characteristics of a stream from a globular cluster. For a larger satellite, it

---

<sup>1</sup>This is usually unique for small angular scales. Sometimes it may be necessary to choose a different independent variable— e.g. if the stream makes a loop on the sky in  $l$ .

is necessary to account for the offset of the stream from the orbit of the satellite (Johnston 1998). It is useful because we can arbitrarily change the number of stars in the stream and their phase distribution in order to explore observational possibilities.

We choose mass loss rates in the range

$$\frac{\dot{M}}{M} \equiv \lambda = 0.1 - 1.0 \times 10^{-10} \text{ yr}^{-1}. \quad (2)$$

The mass loss rates imply that clusters have lost roughly 40 – 60% of their initial mass for fixed  $\lambda$ . The average rate is consistent with (and even somewhat lower than) recent calculations of the evolution of relatively low mass clusters:  $M_c \lesssim 10^5 M_\odot$  (Gnedin & Ostriker 1997; Murali & Weinberg 1997; Johnston, Sigurdsson & Hernquist 1998). For convenience, we define the parameter  $\lambda_{-10}$  to have units  $10^{-10} \text{ yr}^{-1}$  so that  $0.1 \lesssim \lambda_{-10} \lesssim 1$ . We assume a mean stellar mass  $\langle m \rangle = 0.5 M_\odot$  for the cluster to define the number of stars in the stream. The importance of the stellar content of the stream is discussed below.

### 3. Using tidal streams for mass and potential determinations

We develop two methods which can be used to determine the mass and potential of the Galaxy using tidal streams. The first method assumes that a tidal stream very nearly follows a streamline in the Galactic potential, which is a very good approximation for a globular cluster. With complete phase space data for stream stars, we can determine the Galactic mass and potential directly from the observations without any modeling. This approach is a generalization of rotation-curve mass measurements to non-circular orbits. The upcoming space astrometry missions, SIM and GAIA, promise to give phase-space coordinates for nearby clusters ( $d \lesssim 5 \text{ kpc}$ ) and their tidal streams which will be sufficiently accurate to use this method effectively.

The second method involves fitting a model stream curve to stream data where we know the full position and velocity information for the cluster but only know projected positions and radial velocities for stream stars. Here we are motivated by the possibility of combining the results of various plate measurement programs (e.g. Dinescu et al 1999) and the Hipparcos results on globular cluster proper motions (Odenkirchen et al 1997) with current ground-based observational capabilities. We discuss the possibilities in more detail below.

#### 3.1. The streamline approximation

Tidal streams approximately trace the orbit of their parent satellite in the Galaxy. With full phase space information, Lynden-Bell (1982), Kuhn (1993) and Johnston et al (1998) point out that we can approximately measure the potential difference along the stream by measuring the kinetic energy difference between different positions since the force field is conservative. For

globular clusters, the streamline approximation should be quite accurate since the energy spread in the stream is quite small.

For completeness, we present the basic derivation of the equation of energy conservation (Bernoulli’s equation) for a streamline starting with the equation of motion. The acceleration of a particle in a gravitational potential is given by Newton’s law:

$$\frac{d\mathbf{v}}{dt} = -\nabla\Phi(\mathbf{r}). \quad (3)$$

Because the orbit is parameterized by time, this equation provides little information about the potential of the Galaxy. However, rewriting it in Lagrangian form (assuming a static potential),

$$\frac{d\mathbf{v}}{dt} = \frac{\partial\mathbf{v}}{\partial\mathbf{r}} \cdot \frac{d\mathbf{r}}{dt} = \frac{\partial\mathbf{v}}{\partial\mathbf{r}} \cdot \mathbf{v} = -\nabla\Phi(\mathbf{r}), \quad (4)$$

we parameterize the motion in terms of the path of the particle. The acceleration of the particle may therefore be determined from the velocity history of the particle along the path.

While the path of an individual star is unknown, a tidal stream traces the path of a hypothetical particle in the Galactic potential. Since we can, in principle, determine positions and velocities of material along the stream, we can calculate the acceleration at a point using equation (4).

Equation (4) is equivalent to the equation of motion for an element of an incompressible fluid in a static potential (Batchelor 1967). In this context, we may view a tidal stream as the manifestation of a streamline. By observing the velocity field along the streamline, we can determine the gravitational potential which produces it.

With no symmetry assumption, we can obtain general expressions which define the potential along the path. Taking the line integral of equation (4) along the path, we determine the potential difference between two points along the curve

$$\Phi(\mathbf{r}_1) - \Phi(\mathbf{r}_0) \equiv \Delta\Phi_{01} = - \int_{\mathbf{r}_0}^{\mathbf{r}_1} d\mathbf{r} \cdot \frac{\partial\mathbf{v}}{\partial\mathbf{r}} \cdot \mathbf{v}. \quad (5)$$

Since the velocity field is irrotational (except for the possibility of contamination by binaries and spin in the satellite itself), this can be written

$$\Delta\Phi_{01} = - \int d\mathbf{r} \frac{dv^2/2}{d\mathbf{r}} = \frac{1}{2}[v^2(\mathbf{r}_0) - v^2(\mathbf{r}_1)]. \quad (6)$$

This is simply a statement of energy conservation (Bernoulli’s equation) but makes the point that a measurement of the difference in the kinetic energy of two points along the stream is equivalent to a measurement of the potential difference or work done between the two points. Thus, if we can measure an ensemble of tidal streams, we will be able to reconstruct the Galactic potential in a fairly unbiased manner.

Now, assuming a spherically symmetric potential, we easily obtain the mass from the velocity gradient:

$$M(r) = -\frac{r^2}{G} \mathbf{v} \cdot \frac{\partial \mathbf{v}}{\partial \mathbf{r}} \cdot \hat{\mathbf{r}}. \quad (7)$$

For measurement purposes, the equation of energy conservation provides a more convenient way to estimate the spherical mass. Rewriting  $\mathbf{v} \partial \mathbf{v} / \partial \mathbf{r}$  assuming zero vorticity, we find

$$M(r) = -\frac{r^2}{G} \frac{\partial v^2 / 2}{\partial \mathbf{r}} \cdot \hat{\mathbf{r}}. \quad (8)$$

For a circular orbit, we recover the usual formula for rotation curve measurements:

$$M(r) = \frac{r v_c^2}{G}, \quad (9)$$

where  $v_c$  is the circular rotation velocity.

By considering only the radial force component in equation (7), we have ignored the information provided in the other directions. In general, accurate determination of the velocity field as a function of 3-dimensional position along the stream directly gives the 3 components of the gravitational acceleration. This, in turn, provides information on the asphericity of the mass distribution. In fact, the non-radial components of the acceleration can be determined most accurately since they only depend on differences of angular coordinates, which are determined very accurately. For complete generality, we can simply take the divergence of equation (4) and obtain a dynamical form of Gauss' law:

$$\nabla \cdot \frac{\partial \mathbf{v}}{\partial \mathbf{r}} \cdot \mathbf{v} = \frac{1}{2} \nabla^2 v^2 = -\nabla^2 \Phi(\mathbf{r}) = -4\pi G \rho. \quad (10)$$

This, of course, has the disadvantage that second derivatives are required so that the data must be very accurate. Thus it does not appear to be of immediate practical use.

### 3.2. Fitting the projected stream

Given the difficulty of obtaining a complete set of data, we suggest a statistical approach to local mass determinations. What we describe is a procedure for fitting a projected tidal stream to the observational data using a  $\chi^2$  estimator. This is similar to the method described by Johnston et al (1998) but only requires projected positions and radial velocities for material along the stream and does not depend on the structure of the satellite.

Suppose we have a satellite with determined position and velocity, and we observe an associated stellar stream for which we can measure only projected positions and radial velocities of individual stars. Given a model mass distribution defined by some set of parameters  $\theta$  and the satellite position and velocity, we can integrate the satellite trajectory forward and backward in phase for each set  $\theta$  and find the trajectory which best fits the stream data. It is straightforward to

use a  $\chi^2$  estimator, choosing Galactic longitude  $\ell$  as the independent, phase variable and Galactic latitude  $b$  and radial velocity  $v_r$  as dependent variables:

$$\chi^2 = \sum_i^N \left( \frac{b_i - b(\ell_i|\theta)}{\sigma_{b,i}} \right)^2 + \sum_i^N \left( \frac{v_{r,i} - v_r(\ell_i|\theta)}{\sigma_{v,i}} \right)^2; \quad (11)$$

as usual, this defines the logarithm of the joint probability<sup>2</sup> of measuring  $b_i$  and  $v_{r,i}$  at  $\ell_i$ , given the model. Note that it is straightforward to generalize this procedure when more information is available.

The dispersions  $\sigma_{b,i}$  and  $\sigma_{v,i}$  include contributions from the width and velocity dispersion in the stream and uncertainties in the observations. Observational uncertainties are negligibly small for  $\sigma_{b,i}$  but potentially dominate  $\sigma_{v,i}$ . In addition to the physical dispersion in position and velocity, the angular length of the observed stream and the number of stars observed strongly determine the quality of the mass determination. We consider the role of these factors below.

### 3.2.1. Including proper motion uncertainties

In presenting the  $\chi^2$ -estimator, we have implicitly assumed that all available data are determined to high precision. In general, this may not be the case: indeed, we currently face fairly broad uncertainties in proper motion measurements for individual clusters. It is, nevertheless, straightforward to include measurement uncertainties in the curve-fitting procedure from a Bayesian point of view.

For the specific example of proper motion uncertainties, we can add two parameters to our model: namely  $\mu_\alpha$  and  $\mu_\delta$ , the proper motions measured with respect to right ascension and declination, respectively. Since we have estimates and uncertainties for these two quantities, by Bayes' theorem (e.g. Martin 1971) the probability of the model given the data becomes

$$P(\theta') \propto \prod_i P_i(\theta') P(\mu_\alpha) P(\mu_\delta); \quad (12)$$

in other words, the relative probability of any set of parameters  $\theta'$ , given the data, is the joint probability of the data given the model,  $\prod_i P_i(\theta') = \exp(-\chi^2/2)$  multiplied by the prior probabilities of the proper motions,  $P(\mu) = \exp[-(\mu - \mu_0)^2/\sigma_\mu^2]$ , where  $\mu$  denotes either  $\mu_\alpha$  or  $\mu_\delta$  and  $\mu_0$  the respective mean. To return to the original set of parameters  $\theta$ , we project over  $\mu_\alpha$  and  $\mu_\delta$ :

$$P(\theta) \propto \int d\mu_\alpha d\mu_\delta P(\theta'). \quad (13)$$

We examine the influence of proper motion uncertainties in §4.2.1.

---

<sup>2</sup> Strictly speaking, this is the joint probability *density*



#### 4. Mass estimates in spherical potentials

For illustrative purposes, it is simplest to adopt spherical, scale-free mass models for the Galaxy:

$$M(< r) = M_0 \left( \frac{r}{r_0} \right)^\alpha, \quad (14)$$

where  $M_0$  is the mass interior to some assumed radius  $r_0$  and  $\alpha$  gives the slope of the cumulative mass distribution. The model has two parameters  $M_0$  and  $\alpha$ .

In the discussion, we point out several candidate clusters to which we can apply the spherical mass estimator discussed here. Among these are Pal 5: for definiteness in specifying satellite initial conditions, we adopt the best estimates for the space motion for Pal 5. Pal 5 is a low mass globular cluster,  $M_c \sim 10^4 M_\odot$ , at high Galactic latitude and distance  $d = 20$  kpc on the far side of the Galactic center with a fairly elongated orbit. There are two conflicting proper motion determinations (Cudworth & Majewski 1993; Scholz et al 1998) but both indicate that this cluster has just passed apogalacticon and is not associated with the Sgr dwarf galaxy as had been suggested by Ibata et al (1997).

Here we adopt the more recent proper motion  $(\mu_\alpha, \mu_\delta) = (-1.0 \pm 0.3, -2.7 \pm 0.4)$  mas/yr and 3-dimensional velocity determined by Scholz et al (1998; see their Table 2) and integrate the orbit in a spherical potential as defined above with  $M_0 = 2 \times 10^{11} M_\odot$ ,  $r_0 = 20$  kpc and  $\alpha = 1$  (singular isothermal sphere). The orbital period is  $2.4 \times 10^8$  yr. We convert to galactocentric quantities using the formulae given in Johnson & Soderblom (1987), assuming a solar distance  $R_\odot = 8.5$  kpc, a rotation velocity of 220 km/s and the ‘basic solar motion’ (Mihalas & Binney 1982). Although the Galactic mass distribution along the entire orbit is not spherical, we are only interested in the prospects for mass determination from observations on relatively small angular scales:  $\lesssim 10^\circ$ . The stream material over this angular range remains high above the Galactic plane and extends roughly 5 kpc in length so that deviations from spherical symmetry will be small.

##### 4.1. With full phase space information

Here we generate an example stream using an N-body simulation to see if the mass is recovered correctly. Figure 1 shows that we do obtain the correct mass. In this case, the satellite orbit was started 5 radial periods in the past (approximately 1.2 Gyr) so that there have been 5 perigalactic passages. Most of the mass loss occurred in the first passage, so that material has had time to drift away from the satellite, spreading over an angular extent  $|\Delta\Theta| < 3^\circ$ . This is advantageous because, near the satellite, the stream stars have more complicated dynamics since they are still far their asymptotic energy distribution; mass determinations using particles near the satellite will be biased. Distances greater than twice the tidal radius should be adequate to ensure the proper behavior.

In general, measuring the potential difference between two points along a stream is easiest

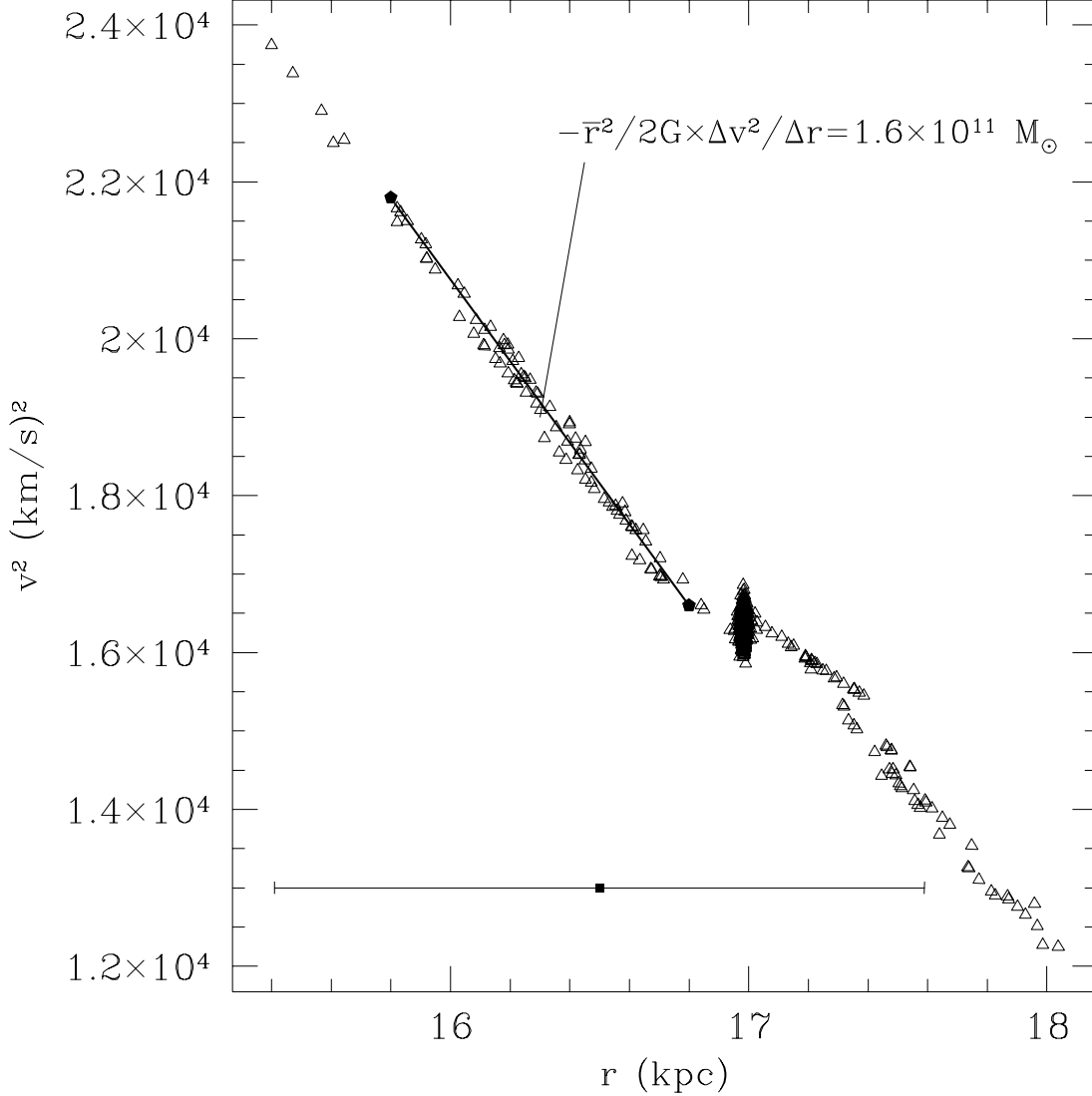


Fig. 1.— A plot of the total square velocity vs. galactocentric radius for a simulated cluster when full information is available for the stream. The plot gives the mass directly. Note that the leading (left) and trailing streams have energy offsets relative to the satellite but a mass determination on either side gives the correct mass. The stream has an angular extent  $|\Delta\Theta| < 3^\circ$  about the satellite. The error bar shows the  $\pm 1 - \sigma$  uncertainty in the SIM and GAIA distance determinations for a satellite at  $d \sim 20$  kpc. Here uncertainties dominate the measurement. The method is effective at smaller distances since the uncertainties shrink quadratically with distance while the length of the stream drops linearly for fixed angular size.

because we need only compute the kinetic energy difference. The mass determination is somewhat more difficult because we must measure velocities at neighboring points and then take differences between these two points to evaluate the derivative. Clearly this can be sensitive to noise. Here,  $v^2$  happens to have an approximately linear dependence on  $r$  so determining the slope is easy. In general, the relationship will be more complicated since  $\Delta v^2 \propto \Delta \Phi$ . One approach would be to fit a smooth curve to the data and use that to extract physical quantities.

Figure 1 shows that at the distance of Pal 5, the uncertainties in distance measurements for SIM and GAIA will dominate since  $\sigma_d \approx (d/20 \text{ kpc})^2 1.6 \text{ kpc}$ . Thus, although absolute distances are known with 10% accuracy, the relative distances of stream stars can be highly uncertain. Since the uncertainties decrease quadratically with distance, the uncertainties in relative distance between stream stars decrease linearly with distance for fixed angular size. This suggests that the method can be best used for fairly nearby clusters,  $d \lesssim 5 \text{ kpc}$ , to determine the 3 components of the gravitational acceleration near the disk.

#### 4.2. In projection

For convenience, we use the Gaussian approximation described above to generate realizations of streams in projection. As a simple check, we compare the results of an N-body simulation with a stream generated using this procedure. The simulation was started 3 radial periods in the past so that the satellite has had 3 perigalactic passages. The realization has phase dispersion  $\sigma_t = 5 \times 10^6 \text{ yr}$ , line-of-sight, radial velocity dispersion  $\sigma_{V_r} = 1 \text{ km s}^{-1}$  and latitude dispersion  $\sigma_b = 10'$ . The phase dispersion  $\sigma_t$  is chosen simply by inspection of the N-body simulation. The others are defined by the characteristics of Pal 5. Figure 2 shows that the agreement is reasonable.

Our view of a tidal stream is determined by the mass loss history of the satellite as well as the angular extent of the observations. If little mass loss has occurred recently, then material will be well mixed and more difficult to detect near the satellite. As an example, Figure 3 shows the observed characteristics of a stream with 56, fully phase-mixed stars in an angular range  $|\Delta\Theta| < 10^\circ$ .

This provides somewhat of a worst-case scenario because there has been no recent mass loss and because there are very few stars in the stream. Nevertheless, although the orbits have indistinguishable spatial projections for all values of  $M_0$  on this scale, the radial velocities provide a strong discriminant. This is not surprising since, physically, the measured mass depends sensitively on the velocities:  $M \propto v^2$ .

To quantify this statistically, we generate fits to streams using the orbit estimator, equation (11). Figure 4 shows the confidence intervals in the  $\alpha - M_0$  parameter space for the indicated particle number and  $\Delta\Theta$  with fully phase-mixed debris. These results suggest that under extremely poor conditions, the mass determination is highly uncertain; under somewhat better conditions it is possible to constrain the mass and mass distribution with several % accuracy.

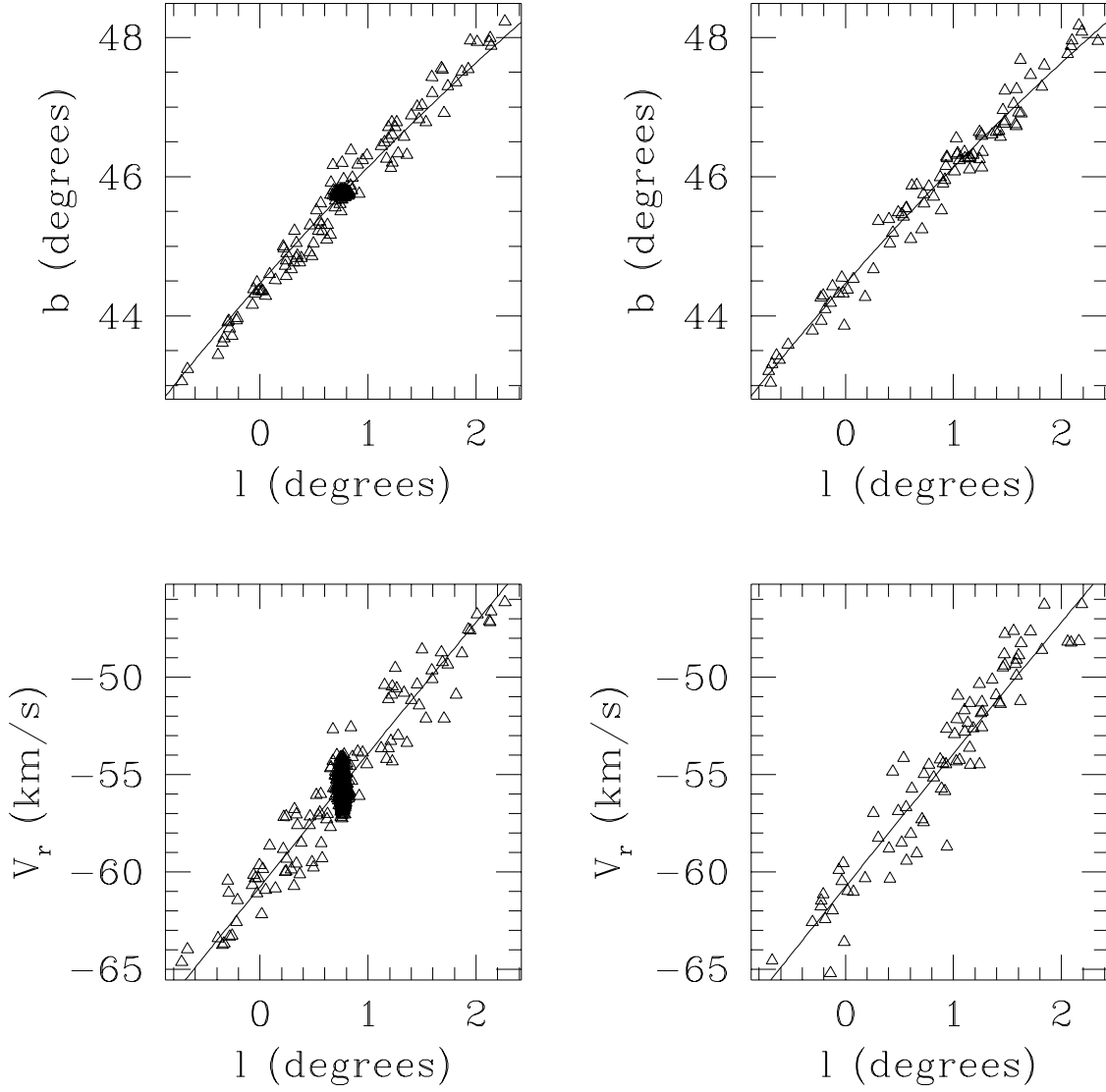


Fig. 2.— Comparison of projected characteristics of N-body tidal stream and Gaussian realizations. The left panels show the  $b$  vs.  $l$  dependence (top) and  $V_r$  vs.  $l$  (bottom) dependence for the N-body stream. The right panels show the same dependences for the approximation. The solid lines in each panel show the projection of the satellite orbit in  $b$  vs.  $l$  and  $V_r$  vs.  $l$ . The agreement is reasonable.

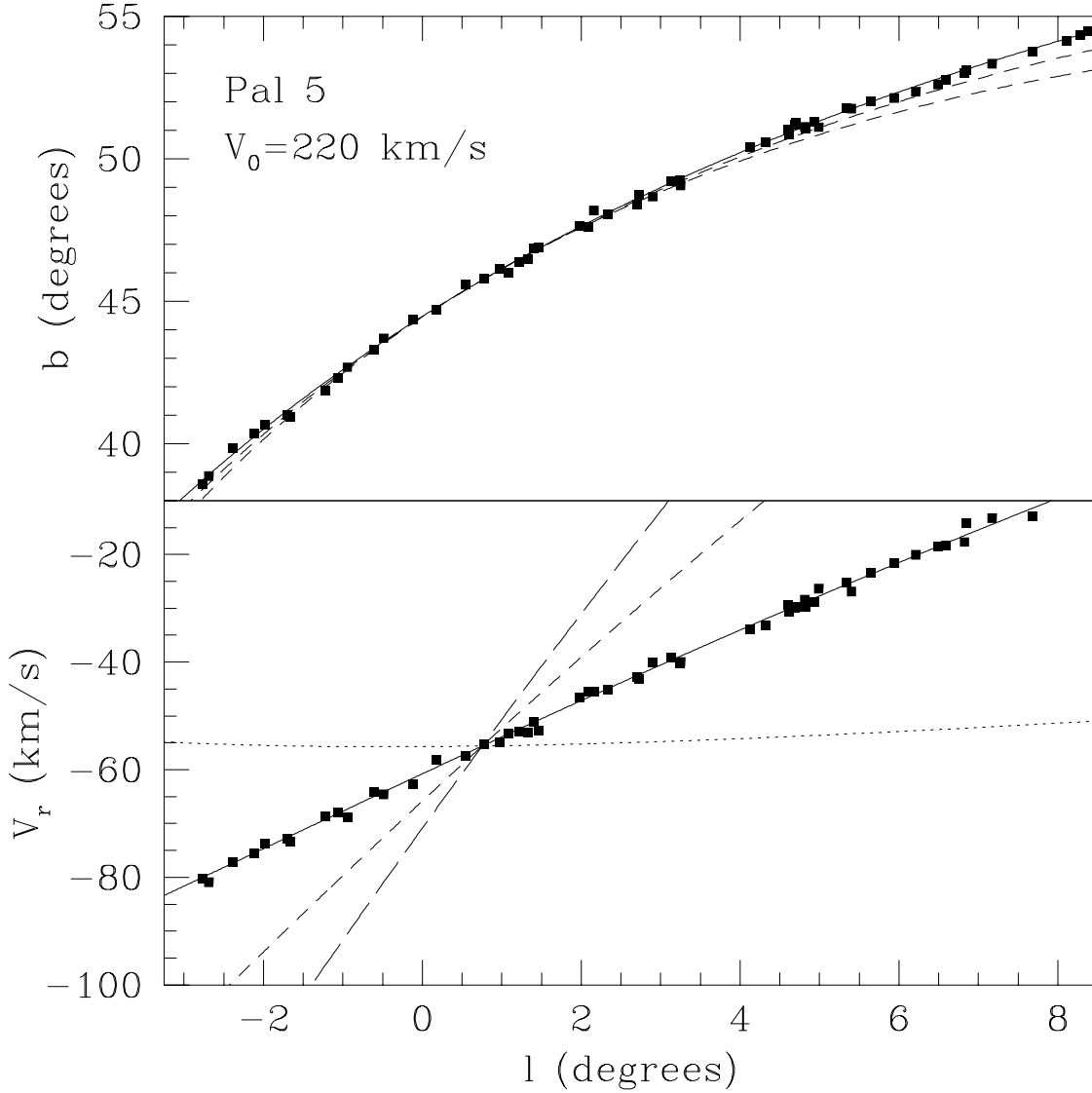


Fig. 3.— Observed characteristics of phase-mixed tidal stream with  $|\Delta\Theta| < 10^\circ$ . There are 56, fully phase-mixed stars in the stream. The cluster sits at the intersection of the curves. The top panel shows  $b$  versus  $l$  for Pal 5 initial conditions and  $M_0 = 1$  (dotted), 2 (solid; actual value), 3 (short dashed) and 4 (long dashed)  $\times 10^{11} M_\odot$ . The bottom panel shows the heliocentric radial velocity versus  $l$  for the stream and each of the different orbits. The radial velocity profile provides a strong discriminant for the mass normalizations.

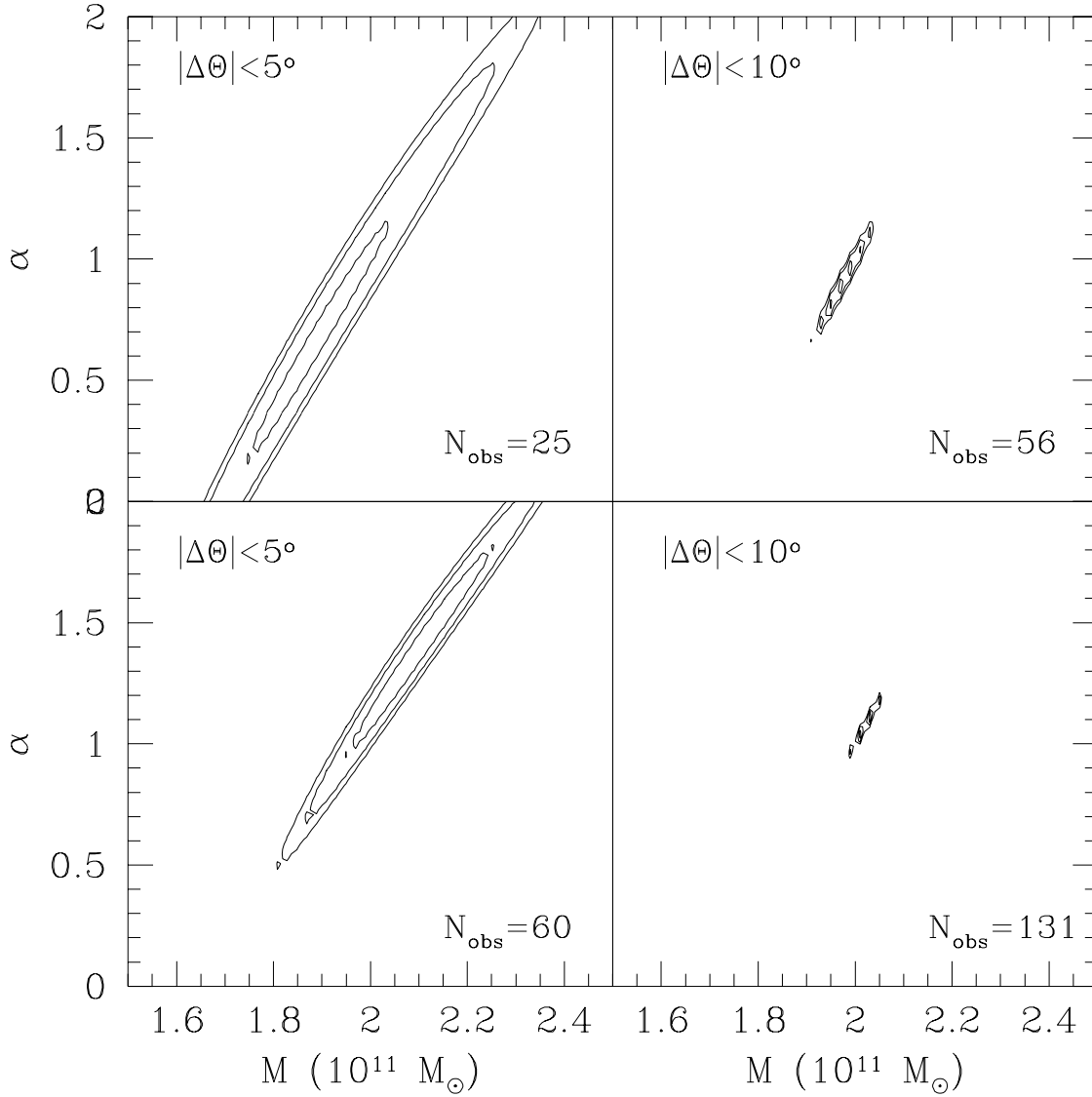


Fig. 4.— Confidence intervals in  $\alpha$  and  $M_0$  for different values of  $\Delta\theta$  and  $N_{\text{obs}}$  in phase-mixed streams. Contours show the 99%, 95% and 68% confidence contours. The upper-left gives the worst-case scenario: very small mass loss in the distant past and a small observed angular scale. The lower-right gives a much better scenario: a factor of 2 increase in mass loss and a factor of 2 increase in angular extent of observations. In the first case, the mass and mass distribution are both highly uncertain, In the latter case, the confidences improve significantly: both  $M_0$  and  $\alpha$  can be determined to within several %. Comparing the upper-right and lower-left panels suggests that larger angular extent improves the mass determination more than does increased sample size.

Assuming fully phase-mixed debris is equivalent to assuming no recent mass loss. As another example, we assume a low rate of mass loss  $\lambda_{-10} = 0.125$  over the last 10 perigalactic passages (roughly 2.5 Gyr) so that debris still clusters near the satellite and has a smaller angular extent. Figure 5 shows the appearance of the stream in projection at the present time over an interval  $|\Delta\Theta| < 10^\circ$ .

Figure 6 shows that a fit to this realization gives fairly tight confidence surfaces but only somewhat stronger than the phase-mixed,  $\lambda_{-10} = 0.5$ ,  $|\Delta\Theta| < 5^\circ$  fit given in Figure 4 (lower left). Although there are 4 times as many stars in this fit, most of them are clumped near the satellite: this nullifies the leverage of the additional stars. The angular extent provides the most leverage in fitting the projected orbit.

#### 4.2.1. The effect of proper motion uncertainties

For illustrative purposes, we have so far assumed that available measurements are perfect: i.e. that there are no uncertainties in these quantities. To be more realistic, we can apply the Bayesian approach presented in §3.2.1 to account for measurement uncertainties. At present, proper motion uncertainties dominate, especially for Pal 5: here we consider their effect on the estimated mass.

Table 1 shows how confidences in the estimated value of  $M_0$ , denoted  $\bar{M}$ , change when we include proper motion uncertainties in the fits. Proper motion uncertainties are defined relative to the mean measured proper motion: *actual* refers to the uncertainties given by Scholz et al. (1998). The error bars  $\sigma_{\bar{M}}$  define 95% confidence intervals about  $\bar{M}$ .

As the table shows, 1% proper motion uncertainties have little effect on the fit: the mass estimate is unbiased and has tight, symmetric confidence levels which are Gaussian. However, as we decrease the proper motion accuracy, the fits degrade and estimates of  $M_0$  appear to become biased to lower values and confidences become highly skewed. Qualitatively, the biasing

Table 1: Estimated  $M_0$  and errors with proper motion uncertainties

$\sigma_{pm}$ (rel.)	$\bar{M}(10^{11} M_\odot)$	$\sigma_{\bar{M}}(10^{11} M_\odot)$	$\Delta\Theta$
1%	2.0	$\pm 0.2$	$5^\circ$
10%	1.7	$\pm_{0.2}^{0.5}$	$5^\circ$
actual	1.4	$\pm_{0.3}^{0.3}$	$5^\circ$
actual	1.8	$\pm_{0.3}^{0.4}$	$10^\circ$

error bars indicate 95% confidence intervals

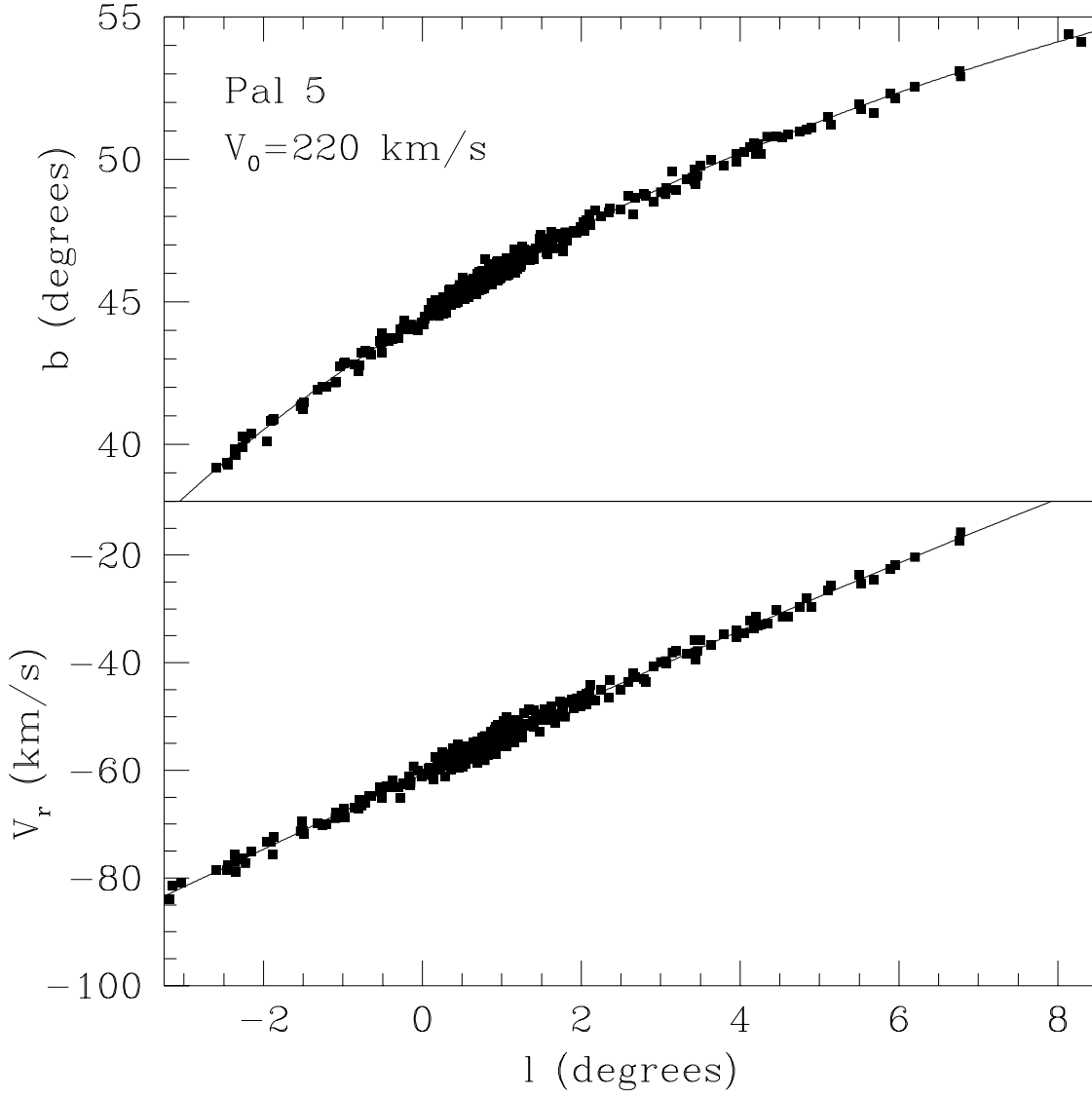


Fig. 5.— Observed characteristics of clumped tidal stream with  $\lambda_{-10} = 0.125$  and  $|\Delta\Theta| < 10^\circ$ . There are 487 stars in the stream. The top panel shows  $b$  versus  $l$  for Pal 5 initial conditions  $2 \times 10^{11} M_\odot$ . The bottom panel shows the heliocentric radial velocity versus  $l$  for the stream and the satellite orbit.



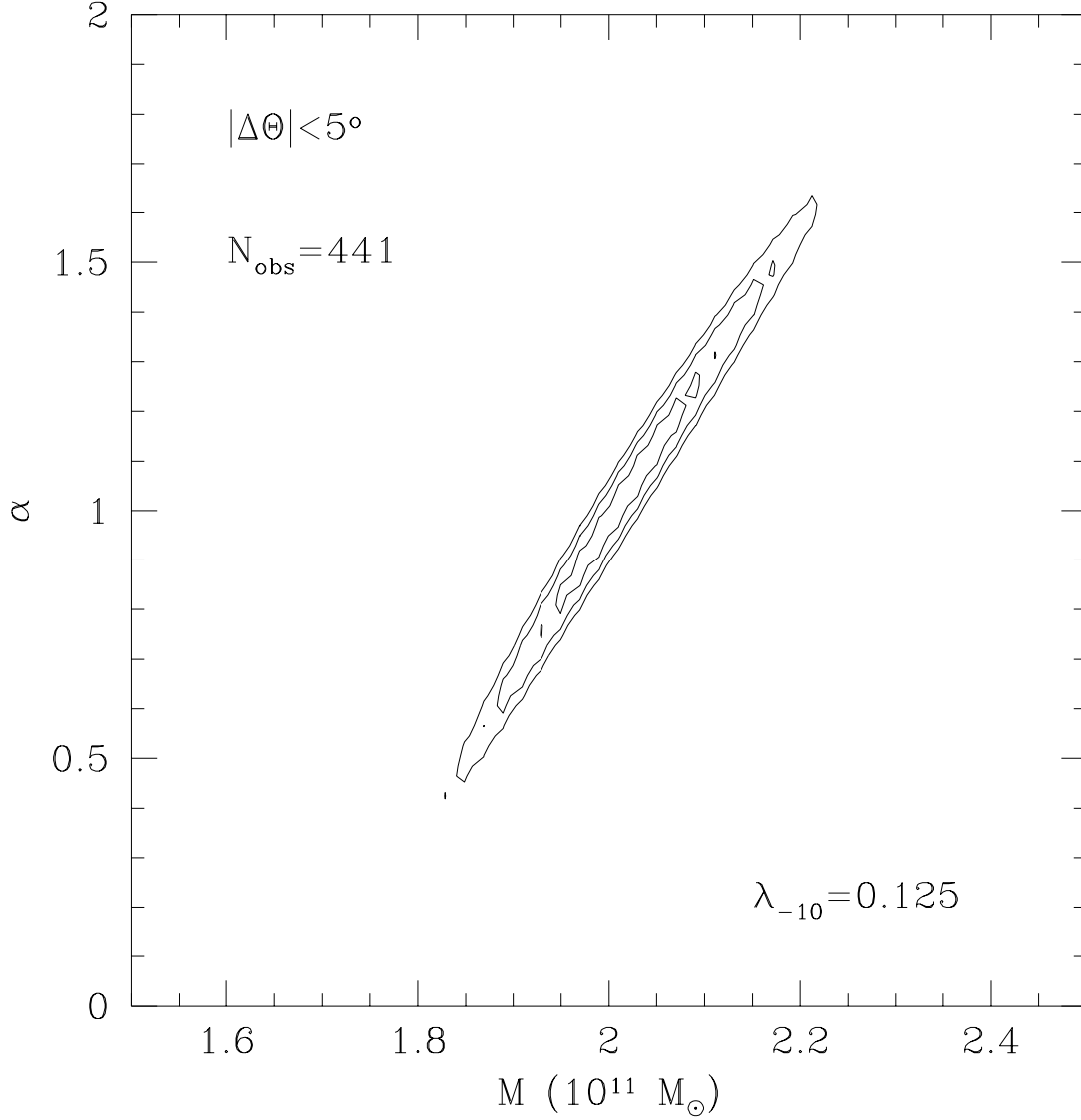


Fig. 6.— Confidence intervals in  $\alpha$  and  $M_0$  for  $|\Delta\Theta| < 5^\circ$  and  $\lambda_{-10} = 0.125$ . Contours show the 99%, 95% and 68% confidence contours. The confidence surfaces are fairly tight but are at nearly the same level as the surfaces for  $N_{\text{obs}} = 60$ ,  $|\Delta\Theta| < 5^\circ$  in the previous figure.

results because, at lower  $M_0$ , there is a broad range of  $(\mu_\alpha, \mu_\delta)$  within the uncertainties which give acceptable fits; at the true value, only a small range gives an acceptable fit. Therefore, in projection, it appears that the lower value of  $M_0$  is more likely. The surfaces cut off rapidly because the range of proper motions giving acceptable fits moves far outside of the range of likely proper motions determined from the observations.

The situation is rather bad for proper motion uncertainties comparable to those which currently plague Pal 5:  $\bar{M}$  is quite far from its true value. By extending the angular length of the observations, the situation improves considerably because differences in orbit become more pronounced over larger angles on the sky. Ultimately, however, the exact nature of this behavior depends on the particular cluster under study and must be considered on a case-by-case basis.

## 5. Discussion and conclusions

We have presented two methods for measuring the mass and potential of the Galaxy using tidal streams from globular clusters. The method with full phase space information is closely related to previous work by Lynden-Bell (1982), Kuhn (1993) and Johnston et al. (1998) and clarifies the idea of using tidal streams as potentiometers. It is both a generalization of rotation curve measurements to non-circular orbits and a dynamical statement of Gauss’ law. In principle, direct measurements of the local gravitational acceleration and density field can be obtained. Of course, it should be emphasized that extremely accurate data are required so current and near-future observations will provide only a limited sample of objects to use with this method.

Analysis of the orbit-fitting method indicates that important preliminary information can be obtained from incomplete phase-space information using current observational capabilities. However, we must be careful to include measurement uncertainties in our analysis. In particular, excessive proper motion uncertainties can introduce biases into estimates. In a broader context, we face the issue of bias in any parametric analysis of the Galactic mass distribution, regardless of measurement error: we must be careful not to ignore systematic biases introduced by adopting any particular model for the Galaxy.

The results presented above suggest that several good candidates in the globular cluster population are available for halo mass determinations at intermediate distances  $R \sim 20$  kpc. These include Pal 5 as mentioned above; NGC 4147, NGC 5024 and NGC 5466 from the Hipparcos sample; and possibly other clusters from ongoing plate measurement programs (e.g. Dinescu et al 1999). These clusters may prove particularly interesting because of their large distance from the Galactic plane: they could provide information on the mass distribution in relatively uncharted territory. Moreover, they provide independent measurements of roughly the same region of the Galaxy because of their spatial proximity.

The Hipparcos sample contains 15 clusters in all. The clusters which we have not mentioned lie closer to the disk and sun and, therefore, have much better proper motion determinations and

are easier to observe. In continuing the work presented here, we will develop detailed models of tidal streams for these clusters in realistic, axisymmetric models of the Milky Way (Kuijken & Dubinski 1995). These clusters will provide excellent candidates for probing the mass distribution very close to the disk. In particular, the astrometric accuracy of the SIM and GAIA satellites within 20 kpc should allow precise distance determinations to clusters and their streams.

There are clearly several uncertainties in the analysis presented above. The principal uncertainty lies in determining cluster mass loss rates, which are difficult to model precisely. A related uncertainty is the stellar content of the stream. On the one hand, low mass clusters provide good candidates because they tend to lose fair amounts of mass through relaxation and tidal heating. However, a large fractional mass loss from a low mass cluster is still a relatively small number of stars. Moreover, the stellar content of the stream will play a strong role in its detectability. Above we adopted  $\langle m \rangle = 0.5M_{\odot}$ , which provides a fair number of stars in the stream. However, at 20 kpc, these stars would have  $I \sim 22$ . It would be extremely difficult– if not impossible– to obtain  $\text{km sec}^{-1}$  radial velocity accuracies for such faint stars. The best that we know of are Vogt et al (1995) radial velocity study of  $I = 18 - 19$  giants in Leo II with Keck which required 10 minute exposures. If, instead, the present mass function has flattened substantially through dynamical evolution (e.g. Pal 5; Smith et al. 1986), then many of the stream stars near the cluster may be bright, higher mass stars. This reduces the number of stream stars for our adopted mass loss rates; but, if the mass loss rate is somewhat higher, the situation may prove ideal.

Proper motions for these distant clusters also remain fairly uncertain in spite of the success of Hipparcos. There is presumably no hope of improving stellar proper motion measurements before the next generation of space-based, astrometric satellites. However, we note that, in the past, there has been some effort to detect water maser emission from giants in globular clusters (Frail & Beasley 1994). Although unsuccessful, the possibility of improving proper motion determinations using VLBI warrants renewed searches with deeper detection limits.

The discussion and analysis presented above suggest that important problems of the structure of the inner Galaxy may be fruitfully addressed by searching for tidal streams from relatively nearby globular clusters. Moreover, with upcoming mission such as SIM (scheduled for 2005) and GAIA (scheduled for 2009), it is essential to establish groundwork for the larger scale studies advocated by Johnston et al (1998) and Zhao et al (1998). We expect that, with present observational capabilities, important progress can be made by focusing attention on the clusters discussed herein. With these missions still relatively far in the future, the progress made now can help resolve important questions and serve as an invaluable guide.

We thank Bill van Altena and the referee, Kathryn Johnston, for helpful discussion and acknowledge support from NSERC and the Fund for Astrophysical Research.

## REFERENCES

- Alcock, C., Allsman, R. A., Alves, D., Axelrod, T. S., Becker, A. C., Bennett, D. P., Cook, K. H., Freeman, K. C., Griest, K., Guern, J., Lehner, M. J., Marshall, S. L., Peterson, B. A., Pratt, M. R., Quinn, P. J., Rodgers, A. W., Stubbs, C. W., Sutherland, W., Welch, D. L., The MACHO Collaboration, 1997, *ApJ*, 486, 697
- Batchelor, G., 1967, *An Introduction to Fluid Dynamics* (Cambridge: Cambridge University Press)
- Debattista, V. & Sellwood, J., 1998, 493, L5
- Dehnen, W. & Binney, J., 1998, *MNRAS*, 294, 429
- Dinescu, D., van Altena, W., Girard, T. & Lopez, C. 1999, *AJ*, 117, 277
- Dubinski, J. & Carlberg, R. 1991, *ApJ*, 378, 496
- Frail, D. & Beasley, A. 1994, *A&A*, 290, 796
- Gnedin, O. & Ostriker, J. 1997, *ApJ*, 474, 223
- Grillmair, C. 1997 in *Galactic Halos: A UC Santa Cruz Workshop*, Ed. D. Zaritsky (ASP: San Francisco), p. 45
- Grillmair, C., Freeman, K., Irwin, M. & Quinn, P. 1995, *AJ*, 109, 2553
- Helmi, A. & White, S. 1999, preprint, astro-ph/9901102
- Ibata, R., Gilmore, G. & Irwin, M. 1994, *Nature*, 370, 194
- Johnson, D. & Soderblom, D. 1987, *AJ*, 93, 864
- Johnston, K. V. 1998, *ApJ*, 495, 297
- Johnston, K. V., Hernquist, L. & Bolte, M. 1996, *ApJ*, 465, 278
- Johnston, K. V., Sigurdsson S. & Hernquist L., 1998, *MNRAS*, 302, 771
- Johnston, K. V., Zhao, H., Hernquist, L. & Spergel, D., 1999, *ApJ*, 512, L109
- Kuhn, J. 1993, *ApJ*, 409, L13
- Kuijken, K. & Dubinski, J. 1995, *MNRAS*, 277, 1341
- Leonard, P. & Tremaine, S. 1990, *ApJ*, 353, 486
- Little, B. & Tremaine, S. 1987, *ApJ*, 320, 493
- Lynden-Bell, D., 1982, *Observatory*, 102, 202
- Kochanek, C. 1996, *ApJ*, 457, 228
- Majewski, S. & Cudworth, K. 1993, *PASP*, 105, 987
- Majewski, S., Munn, J. & Hawley, S. 1996, *ApJ*, L73
- Martin, B. R., 1971, *Statistics for Physicists* (Academic Press: London), p. 213

- Mateo, M., Olszewski, E. & Morrison, H. 1998, *ApJ*, 508, L55
- Mihalas, D. & Binney, J. 1981, *Galactic Astronomy* (Freeman: San Francisco), p. 398
- Moore, B. & Davis, M., 1994, *MNRAS* 270, 209
- Murali, C. & Weinberg, M. D. 1997, *MNRAS*, 291, 717
- Navarro, J., Frenk, C. & White, S. 1997, *ApJ*, 490, 493
- Odenkirchen, M., Brosche, P., Geffert, M. & Tucholke, H. 1997, *New Ast.*, 2, 477
- Scholz, R., Irwin, M., Odenkirchen, M. & Meusinger, H. 1998, *A&A*, 333, 531
- Smith, G., McClure, R., Stetson, P., Hesser, J. & Bell, R. 1986, *AJ*, 91, 842
- Tremaine, S. 1998, preprint, astro-ph/9812146
- Tremaine, S. 1993 in *Back to the Galaxy*, eds. S. S. Holt & F. Verter (AIP Conf. Proc: New York), p. 599.
- Tremaine, S. & Ostriker, J. P. 1998, preprint, astro-ph/9812145
- Vesperini, E. 1997, *MNRAS*, 287, 915
- Vogt, S., Mateo, M., Olszewski, E. & Keane, M. 1995, *AJ*, 109, 151
- Zhao, H., Johnston, K., Spergel, D. & Hernquist, L. 1999, preprint, astro-ph/9901071